Jet quenching review I

Su Houng Lee

Main Review article; hep-ph/0406201

: Leading-particle suppression in high energy nucleus-nucleus collisions

A. Dainese, C. Loizides and G. Paic.

Other Main References:

1. The Landau–Pomeranchuck–Migdal effect in QED, Baier, Dokshitzer, Mueller, Peigne, Schiff (BDMPS), NP B478 (1996) 577
2. Radiative energy loss of high energy quarks and gluons in a finite-volume quark gluon plasma, BDMPS, NPB 483 (1997) 291.
3. Gluon radiation off hard quarks in a nuclear environment: opacity expansion, U. Wiedemann, NPB 588 (2000) 303
4. Calculating quenching weights, Salgado, Wiedemann, PRD 68, 014008 (2003)

Ject quenching

High-momentum leading-particle suppression in nucleus–nucleus (AA) with respect to proton–proton collisions is regarded as one of the major discoveries at the Relativistic Heavy Ion Collider (RHIC), Brookhaven. In Au–Au collisions at centre-of-mass energy $\sqrt{s_{\rm NN}} = 200$ GeV per nucleon–nucleon (NN) pair, the two experiments with high transverse momentum, $p_{\rm t}$, capabilities, PHENIX and STAR, have measured:

- the suppression of single particles at high $p_{\rm t}$ ($\gtrsim 4$ GeV) and central pseudorapidity ($|\eta| \lesssim 1$), quantified via the nuclear modification factor

$$R_{\rm AA}(p_{\rm t}) \equiv \frac{1}{\langle N_{\rm coll}\rangle_{\rm centrality\ class}} \times \frac{{\rm d}^2 N_{\rm AA}/{\rm d}p_{\rm t}{\rm d}\eta}{{\rm d}^2 N_{\rm pp}/{\rm d}p_{\rm t}{\rm d}\eta}, \qquad (1)$$

  which would be equal to unity if the AA collision was a mere superposition of $N_{\rm coll}$ independent NN collisions ($N_{\rm coll}$ scaling); instead, at high $p_{\rm t}$ $R_{\rm AA}$ is found to decrease from peripheral to central events, down to ≈ 0.2 in head-on collisions [1, 2]; the suppression is the same for charged hadrons and neutral pions for $p_{\rm t} \gtrsim 5$ GeV;
- the disappearance, in central collisions, of jet-like correlations in the azimuthally-opposite side of a high-$p_{\rm t}$ leading particle [3];
- the absence of such effects in d–Au collisions at the same energy [4, 5].

An important parameter to be understood $< \hat{q} >$

Section 2

σινγερ≅πηψα.σνυ.αχ.κρ>

Parton energy loss and collision goemetry

+My personal review

Basics: fast charged particle scattering from scattering centers

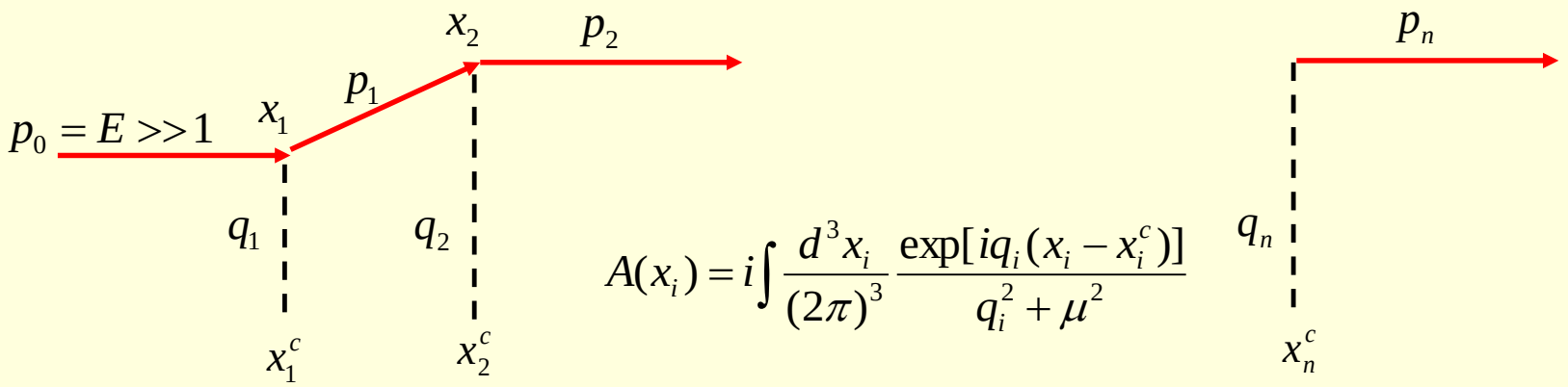

$$S = < p_n | \frac{i^n}{n!} \int d^4x_n \bar{\psi}(x_n) A^0(x_n) \psi(x_n) ..... \int d^4x_1 \bar{\psi}(x_1) A^0(x_1) \psi(x_1) | p_0 >$$

$$S \propto \delta(p_N^0 - p_0^0) \sum_\sigma \int \prod_{i=1}^{n-1} \frac{d^3p_i}{p_i^2 + i\eta} \prod_{i=1}^{n} \frac{\exp[-iq_i \cdot x_{\sigma(i)}]}{q_i^2 + \mu^2}$$

$$p_i = (E, p_{i,z}, p_{i,T}), \qquad p_i^2 = E^2 - p_{i,z}^2 - p_{i,T}^2$$

$$q_i = p_i - p_{i-1}$$

$$p_{i,z} = E - \frac{p_{i,T}^2}{2E} + i\eta,$$

$$p_{i,z} = -E + \frac{p_{i,T}^2}{2E} - i\eta$$

$$S \propto \delta(p_N^0 - p_0^0) \sum_\sigma \int \prod_{i=1}^{n-1} \frac{d^3 p_i}{p_i^2 + i\eta} \prod_{i=1}^{n} \frac{\exp[-iq_i \cdot x_{\sigma(i)}]}{q_i^2 + \mu^2}$$

$$i\varphi_{scatt} = -i\sum_{i=1}^{n} q_i \cdot x_{\sigma(i)} = -i\sum_{i=1}^{n} q_{i,T} \cdot x_{\sigma(i),T} + i\sum_{i=1}^{n-1} p_{i,z} \cdot (z_{\sigma(i+1)} - z_{\sigma(i)}) + i(p_{0,z} z_{\sigma(1)} - p_{n,z} z_{\sigma(n)})$$

$$\frac{1}{q_1^2 + \mu^2} = \frac{1}{(p_1 - E)^2 + p_{1,T}^2 + \mu^2}$$

$$p_{i,z} = E - \frac{p_{i,T}^2}{2E} + i\eta, \quad \rightarrow \quad \frac{1}{p_{1,T}^2 + \mu^2}$$

$$p_{i,z} = -E + \frac{p_{i,T}^2}{2E} - i\eta \quad \rightarrow \quad \frac{1}{4E^2 + p_{1,T}^2 + \mu^2}$$

1. The high energy electron scatters successively on ordered scattering centers

$$z_{\sigma(n)} > z_{\sigma(n-1)} > \ldots\ldots > z_{\sigma(1)}$$

2. As a consequence, the electron momenta are on shell

$$p_{i,z} = E - \frac{p_{i,T}^2}{2E} + i\eta$$

Basics: fast charged particle radiating from scattering centers

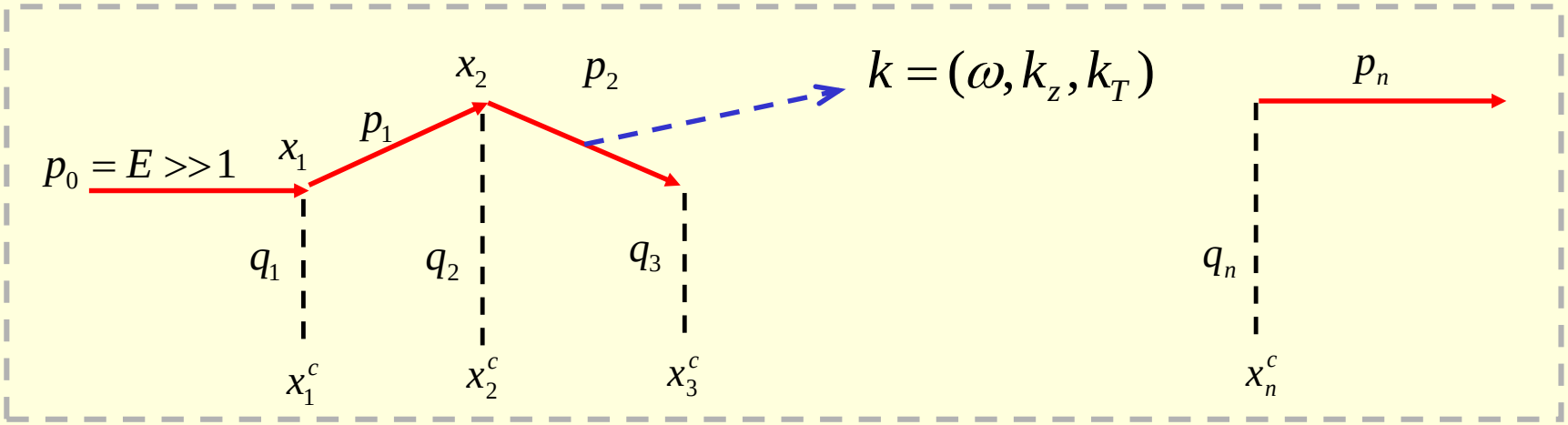

$$\varphi_{rad} = \varphi_{scatt} - \frac{\omega}{2}\sum_{i=j}^{n-1} u_i^2 (z_{i+1} - z_i), \qquad u_j = \frac{k_T}{\omega} - \frac{p_{j,T}}{E}$$

$$\omega \frac{dI}{d\omega} = \frac{\alpha}{\pi^2}\int d\Omega \left\langle \left| \sum_{i=1}^{n} B_i \exp(i\phi_i) \right|^2 \right\rangle$$

For QCD: Non-abelian nature

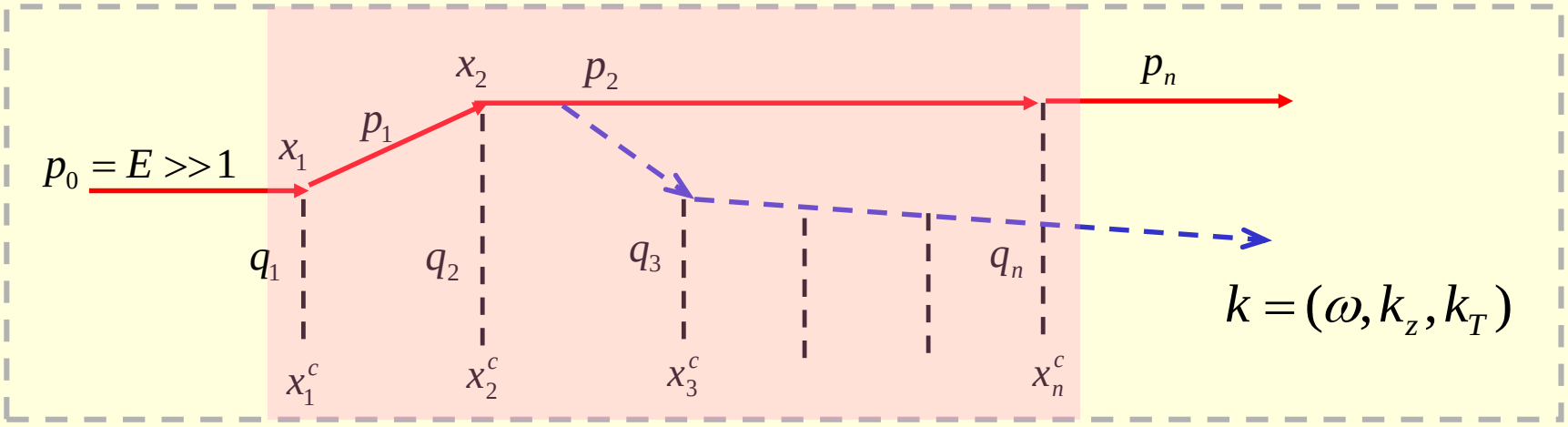

$$\varphi = -<\frac{k_T^2}{2\omega}\Delta z>$$

Two parameters characterizing the medium

$$\hat{q} = \frac{<q_T^2>_{medium-transfer}}{\lambda_{dist-scattering-center}}, \qquad L \Rightarrow QGP-size$$

Characteristic phase for coherent radiation

$$k_T^2 = \mu^2 \frac{L}{\lambda} = \hat{q}L \;\rightarrow\; \varphi = \frac{\hat{q}L}{2\omega}L = \frac{\omega}{\omega_c}$$

Change of variables typically to

$$\omega_c = \hat{q}\frac{L^2}{2}, \qquad R = \frac{2\omega_c^2}{\hat{q}L} = \frac{1}{2}\hat{q}L^3$$

Some famous result for QCD

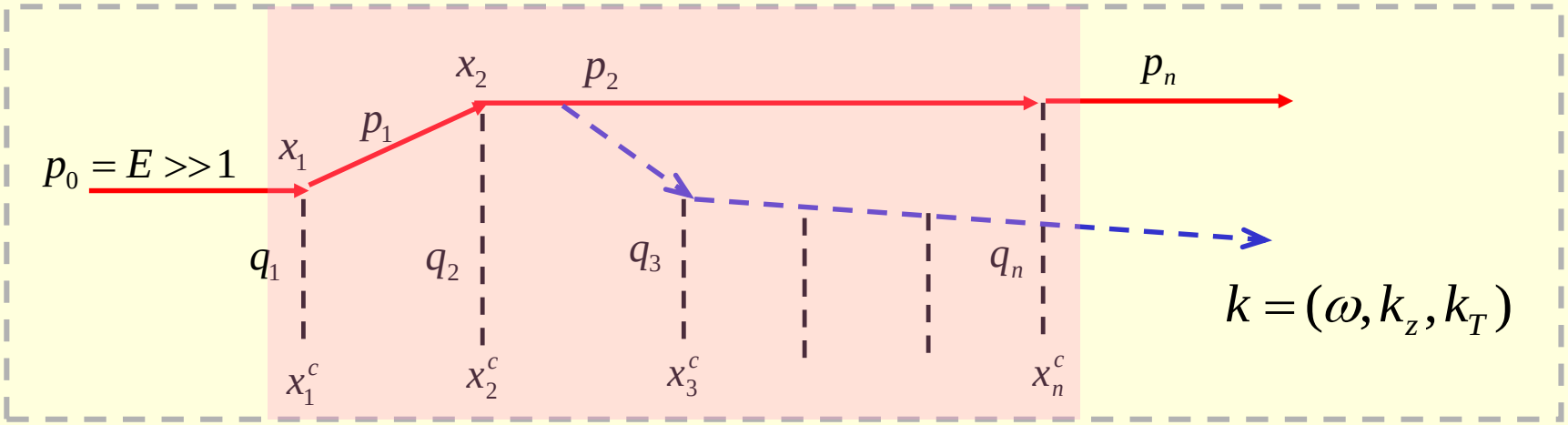

$$\lim_{R\to\infty} \omega \frac{dI}{d\omega} \approx \frac{2\alpha_s C_R}{\pi} \begin{cases} \sqrt{\dfrac{\omega_c}{\omega}} & \text{for} \quad \omega < \omega_c \\ \dfrac{1}{12}\left(\dfrac{\omega_c}{\omega}\right)^2 & \text{for} \quad \omega \geq \omega_c \end{cases}$$

$$\langle \Delta E \rangle_{R\to\infty} = \lim_{R\to\infty} \int_0^\infty \omega \frac{dI}{d\omega} d\omega \quad \propto \quad \alpha_s C_R \omega_c \quad \propto \quad \alpha_s C_R \hat{q} L^2$$

Section 3

Leading-particle suppression procedure

Actual step I: Factorization formula

1. generation of a parton, quark or gluon, with $p_t > 3$ GeV, using the PYTHIA event generator [23] in pp mode with CTEQ 4L parton distribution functions [24]; the p_t-dependence of the quarks-to-gluons ratio is taken from PYTHIA;

$$\left.\frac{d^2\sigma^h}{dp_t dy}\right|_{y=0} = \sum_{a,b,j=q,\bar{q},g} \int dx_a dx_b dz_j \, f_a(x_a) f_b(x_b) \left.\frac{d^2\hat{\sigma}^{ab\to jX}}{dp_{t,j} dy_j}\right|_{y_j=0} \frac{D_{h/j}(z_j)}{z_j^2}$$

Step II: determination of parameters

2. determination of the two input parameters, ω_c and R, for the calculation of the quenching weights, i.e. the energy-loss probability distribution $P(\Delta E)$;

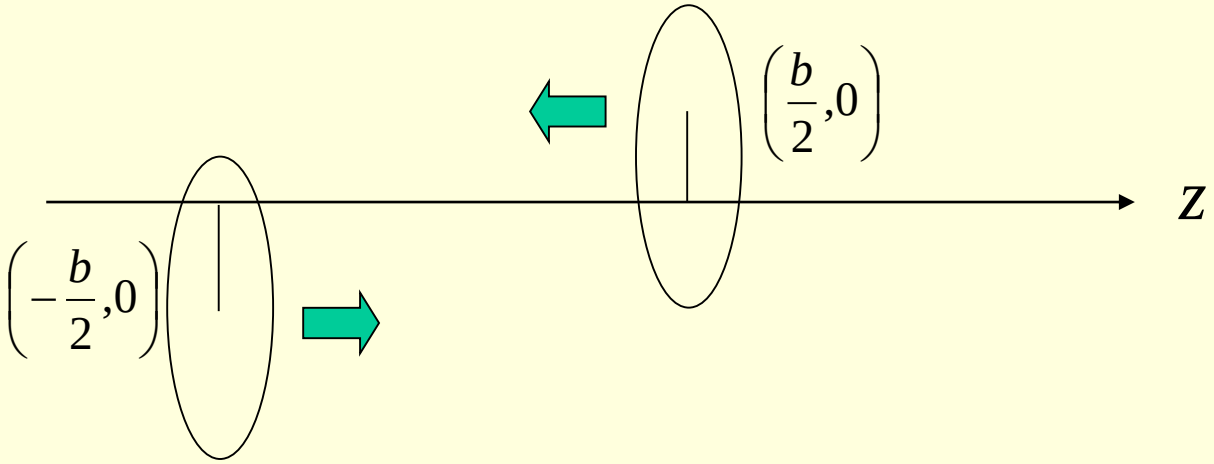

$$\hat{q}(\xi;b) = k \times T_{\rm A}T_{\rm B}(x_0 + \xi\cos\phi_0, y_0 + \xi\sin\phi_0; b)\,,$$

$$T_{\rm A}T_{\rm B}(x,y;b) \equiv T_{\rm A}(x,y) \times T_{\rm B}(x,y) \qquad T_{\rm i}(x,y) \equiv \int {\rm d}z\, \rho_{\rm i}^{\rm WS}(x,y,z).$$

For each parton

$$\omega_{\rm c}\,|_{\rm effective} \equiv \frac{1}{2}\,\langle\hat{q}\rangle\, L^2 = \int_0^\infty \xi\,\hat{q}(\xi)\,{\rm d}\xi \qquad \langle\hat{q}\rangle\, L\,|_{\rm effective} \equiv \int_0^\infty \hat{q}(\xi)\,{\rm d}\xi$$

$$R\,|_{\rm effective} \equiv \frac{2\,(\omega_{\rm c}\,|_{\rm effective})^2}{\langle\hat{q}\rangle\, L\,|_{\rm effective}}\,.$$

Different parameterization

$$L = R/\omega_c = 2\,I_1/I_0 \quad \text{and} \quad \hat{q} = 2\,\omega_c^2/(L\,R) = I_0^2/(2\,I_1)\,.$$

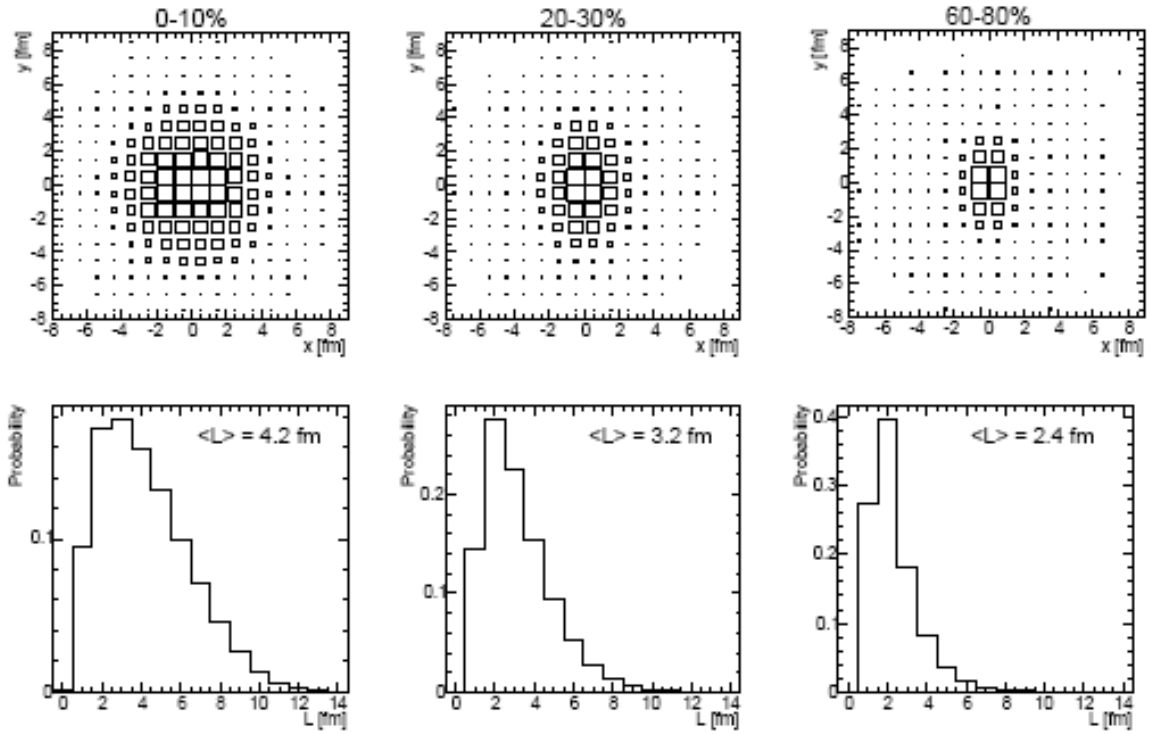

Figure 1: Distributions of parton production points in the transverse plane (upper row) and in-medium path length (lower row) in central, semi-central and peripheral Au–Au collisions. The quantity $\langle L \rangle$ is the average of the path length distribution.

Step III: determination of parameters

3. sampling of an energy loss ΔE according to $P(\Delta E)$ and definition of the new parton transverse momentum, $p_{\mathrm{t}} - \Delta E$;

- *Reweighted:* truncate $P(\Delta E)$ at $\Delta E = E$ and renormalize it to unity by dividing out the factor $\int_0^E \mathrm{d}\epsilon\, P(\epsilon)$. The Monte Carlo implementation of this approach is: sample ΔE from the original $P(\Delta E)$; if $\Delta E > E$, sample another ΔE; iterate until a $\Delta E \leq E$ is sampled.
- *Non-reweighted:* truncate $P(\Delta E)$ at $\Delta E = E$ and add the δ-function $\delta(\Delta E - E) \int_E^\infty \mathrm{d}\epsilon\, P(\epsilon)$ to it. The integral of P is, in this way, maintained equal to one. The corresponding Monte Carlo implementation reads: sample an energy loss ΔE and set the new parton energy to zero if $\Delta E \geq E$.

Step IV: determination of parameters

4. (independent) fragmentation of the parton to a hadron using the leading-order Kniehl-Kramer-Pötter (KKP) fragmentation functions [25].

$$\left.\frac{\mathrm{d}^2\sigma^h_{\mathrm{quenched}}}{\mathrm{d}p_{\mathrm{t}}\mathrm{d}y}\right|_{y=0} = \sum_{a,b,j=\mathrm{q},\bar{\mathrm{q}},\mathrm{g}} \int \mathrm{d}x_a\,\mathrm{d}x_b\,\mathrm{d}\Delta E_j\,\mathrm{d}z_j\, f_a(x_a)\, f_b(x_b)\, \left.\frac{\mathrm{d}^2\hat{\sigma}^{ab\to jX}}{\mathrm{d}p^{\mathrm{init}}_{\mathrm{t},j}\mathrm{d}y_j}\right|_{y_j=0} \times \delta\left(p^{\mathrm{init}}_{\mathrm{t},j} - (p_{\mathrm{t},j} + \Delta E_j)\right)\, P(\Delta E_j; R_j, \omega_{\mathrm{c},j})\, \frac{D_{h/j}(z_j)}{z_j^2},$$

Section 4

Results

Nuclear modification factor in Au-Au at 200 GeV - i

$$R_{\mathrm{AA}}(p_{\mathrm{t}}) \equiv \frac{1}{\langle N_{\mathrm{coll}} \rangle_{\text{centrality class}}} \times \frac{\mathrm{d}^2 N_{\mathrm{AA}}/\mathrm{d}p_{\mathrm{t}}\mathrm{d}\eta}{\mathrm{d}^2 N_{\mathrm{pp}}/\mathrm{d}p_{\mathrm{t}}\mathrm{d}\eta},$$

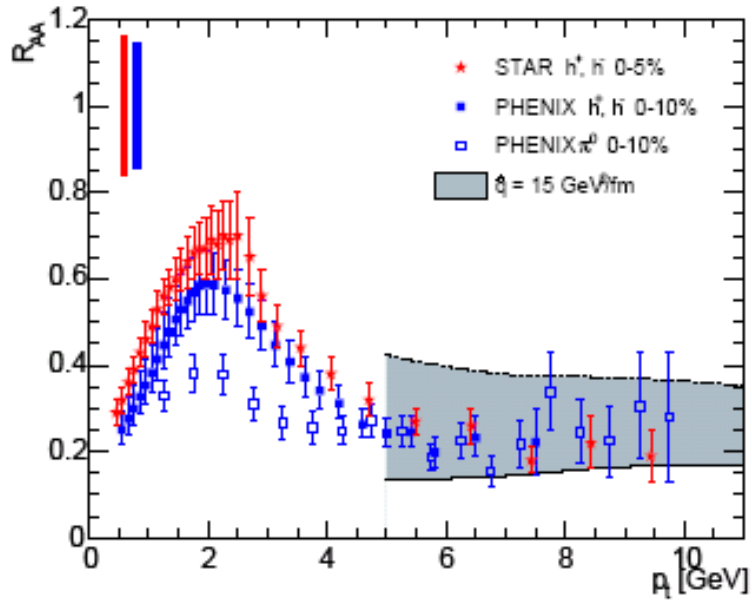

panel) are reported. In the right-hand plot and in all the following figures the shaded band is delimited by *non-reweighted* case (solid line) and *reweighted* case (dashed line).

Nuclear modification factor in Au-Au at 200 GeV - ii

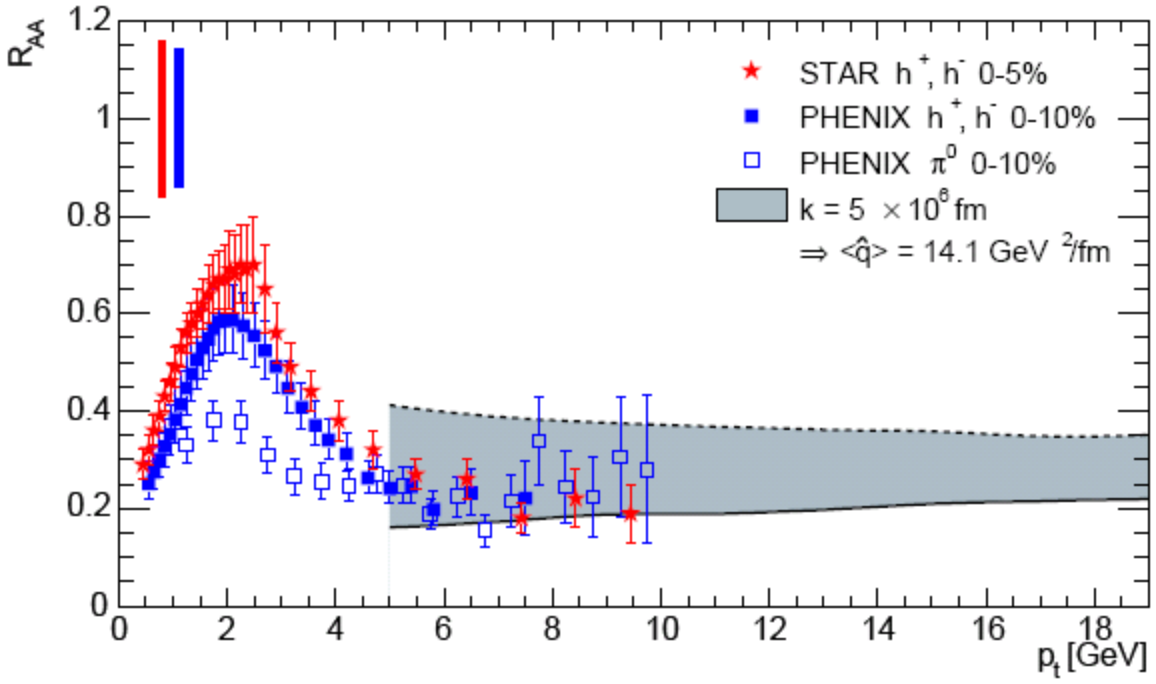

Figure 3: $R_{\mathrm{AA}}(p_{\mathrm{t}})$ for central Au–Au collisions at $\sqrt{s_{\mathrm{NN}}} = 200$ GeV. The model band is obtained with a parton-by-parton calculation of ω_{c} and R. The average transport coefficient is 14 GeV^2/fm.

Nuclear modification factor in Au-Au at 200 GeV - iii

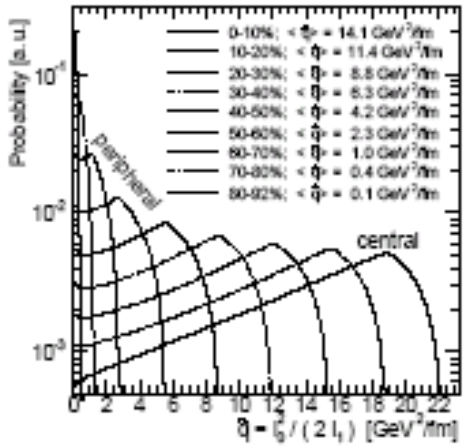

Figure 4: Distributions of $\hat{q}$, calculated from Eq. (16), for different centralities; the k parameter is fixed to the value that allows to describe R_{AA} for the most central collisions.

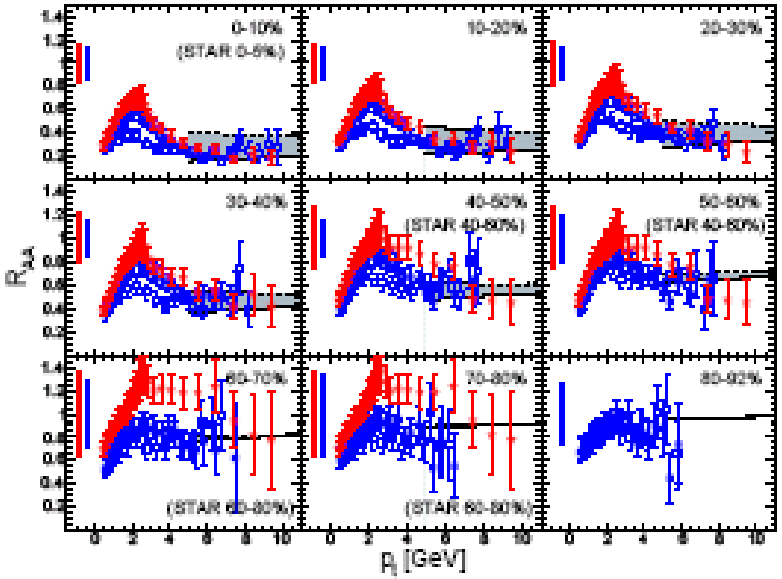

Figure 5: $R_{AA}(p_t)$ for different centralities. Data are PHENIX charged hadrons (closed squares) and π^0 (open squares) [1] and STAR charged hadrons (stars) [2].

Nuclear modification factor in Au-Au at 200 GeV - iv

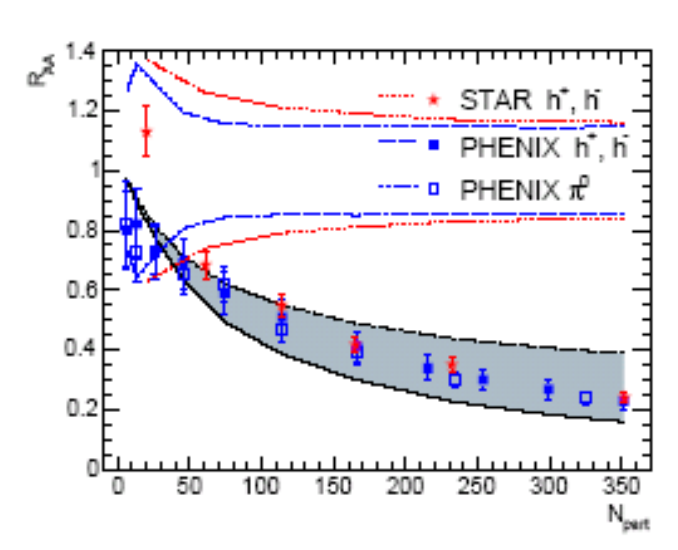

Figure 6: Average R_{AA} in the range $4.5 < p_t < 10$ GeV [1,2]

Back to back correlation

$$D_{\rm AA} = \int_{p_{\rm t}^{\rm min}}^{p_{\rm t,1}} {\rm d}p_{\rm t,2} \int_{\Delta\phi>\Delta\phi^{\rm min}} {\rm d}\Delta\phi \, \frac{{\rm d}^3\sigma_{\rm AA}^{h_1h_2}/{\rm d}p_{\rm t,1}{\rm d}p_{\rm t,2}{\rm d}\Delta\phi}{{\rm d}\sigma_{\rm AA}^{h_1}/{\rm d}p_{\rm t,1}}$$

[28] X.N. Wang, arXiv:nucl-th/0405017.

The STAR data [3] are for trigger particles with $4 < p_{\rm t,1} < 6$ GeV and associated particles with $p_{\rm t,2} > p_{\rm t}^{\rm min} = 2$ GeV and $p_{\rm t,2} < p_{\rm t,1}$, with $\Delta\phi \equiv |\phi_1 - \phi_2| > \Delta\phi^{\rm min} = 130°$. The correlation strength is then corrected for

suppression factor: $I_{\rm AA} = \dfrac{D_{\rm AA}}{D_{\rm pp}}$.

We generate pairs of partons with the same initial $p_{\rm t}$ and separated in azimuth by $\Delta\phi = 180°$. Then, we calculate $\omega_{\rm c}$ and R for each parton and apply energy loss and fragmentation. We count as trigger particle every hadron h_1 with $4 < p_{\rm t,1} < 6$ GeV and as associated away-side particle the other hadron h_2 of the pair, if its transverse momentum is in the range 2 GeV $< p_{\rm t,2} < p_{\rm t,1}$. We define:

$$I_{\rm AA} = \left(\frac{N^{\rm associated}}{N^{\rm trigger}}\right)_{\rm with\ energy\ loss} \Big/ \left(\frac{N^{\rm associated}}{N^{\rm trigger}}\right)_{\rm w/o\ energy\ loss} . \qquad (19)$$

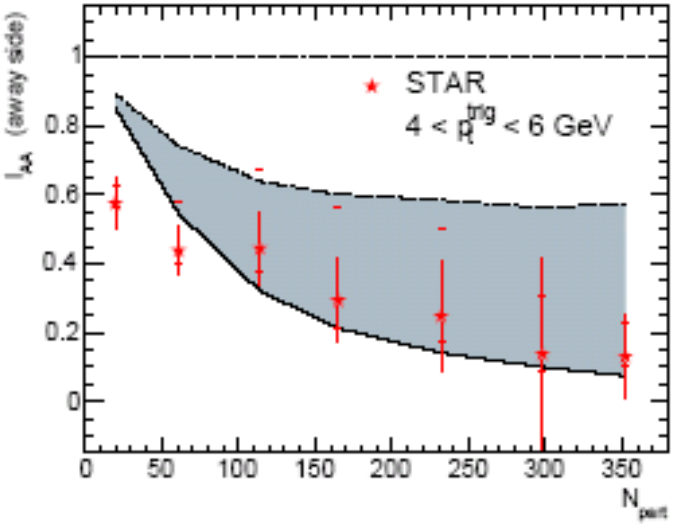

Azimuthally-differential observables - i

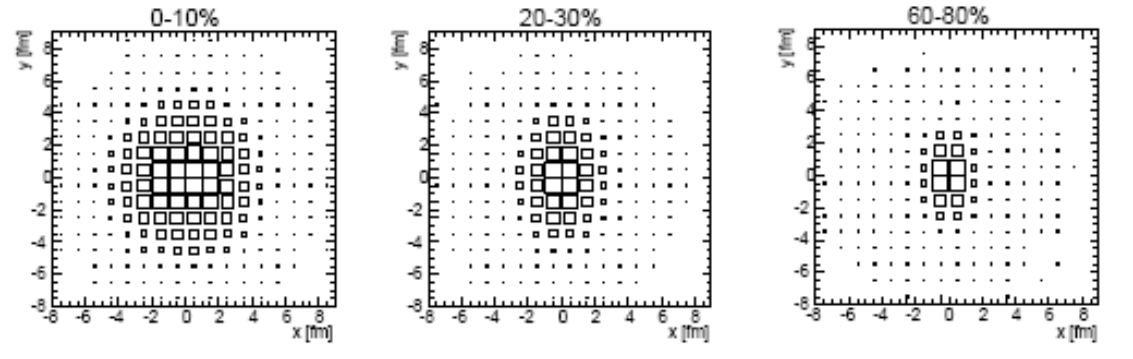

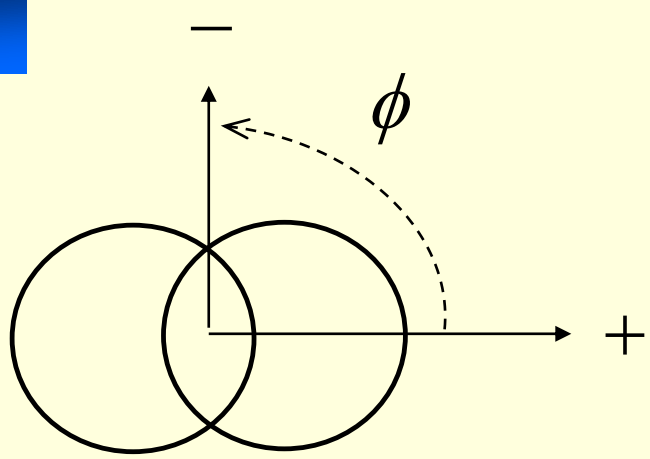

$$a \cdot (1 + 2\, v_2 \cos 2\phi);$$

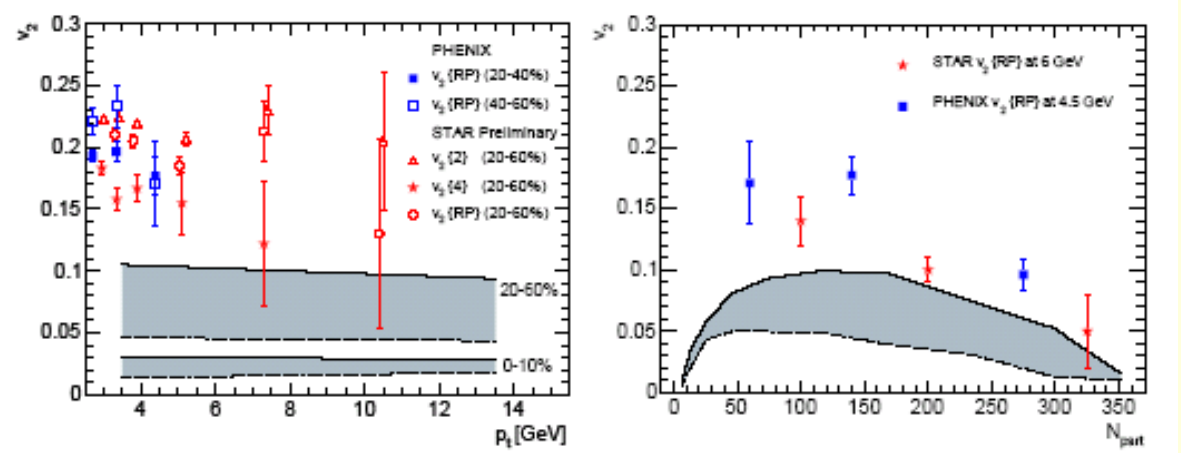

Figure 7: Transverse momentum and centrality dependence of the azimuthal anisotropy v_2, compared to measurements for charged hadrons from PHENIX [30] and STAR [31, 33] (see text). Only the statistical errors are plotted. Note that, opposed to all other figures, here the model result for the *non-reweighted* case (solid) is the upper limit of the band and that for the *reweighted* case (dashed) is the lower one.

Non negligible collective flow effect

Azimuthally-differential observables - ii

- $R_{\rm AA}^{\phi_0}(p_{\rm t})$, the nuclear modification factor for hadrons in an azimuthal cone of 45° centred at the angle ϕ_0 with respect to the event plane; we use $\phi_0 = 0°$ (in-plane), $\phi_0 = 90°$ (out-of-plane) and $\phi_0 = 45°$ (intermediate);
- $I_{\rm AA}^{\phi_0}$ (away side), the nucleus–nucleus away-side correlation strength relative to pp, in the three azimuthal regions defined for $R_{\rm AA}^{\phi_0}$.

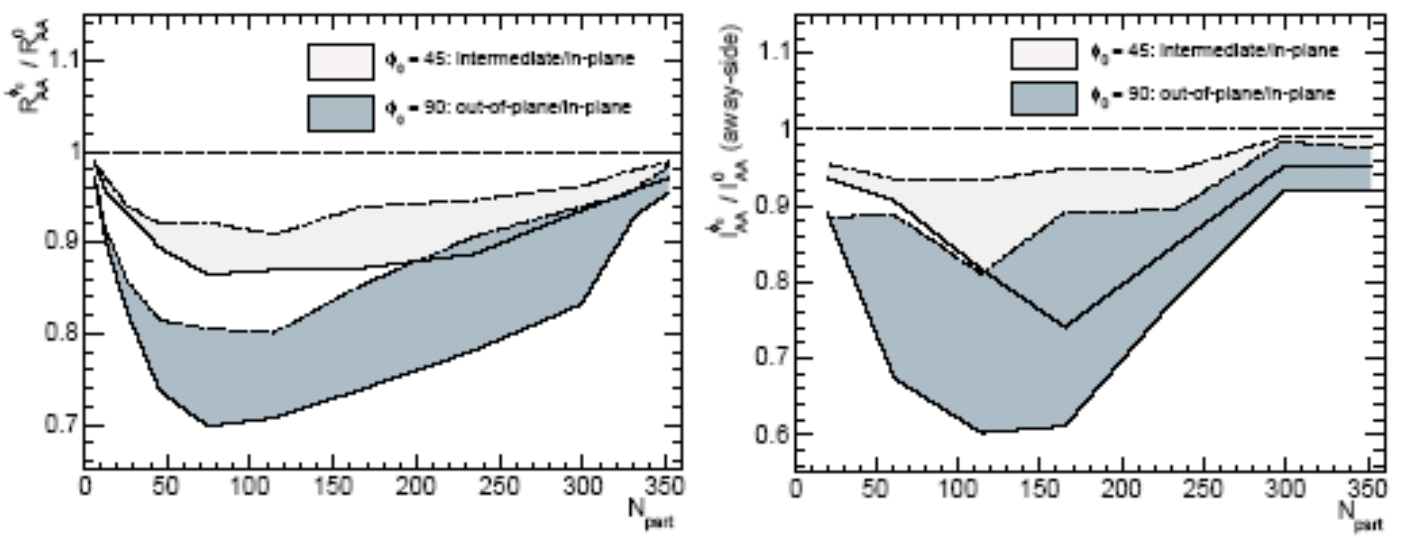

Figure 8: Azimuthal variation of the nuclear modification factor of the away-side correlations. In the left-hand panel, ratios $R_{\rm AA}^{90}/R_{\rm AA}^{0}$ (out-of-plane/in-plane) and $R_{\rm AA}^{45}/R_{\rm AA}^{0}$ (intermediate/in-plane), averaged over the range $4.5 < p_{\rm t} < 10$ GeV. In the right-hand panel, the same ratios for $I_{\rm AA}$ with trigger conditions as in Fig. 6. Both observables are plotted as a function of $N_{\rm part}$.

Nuclear modification factor in Au-Au at 62.4 GeV - i

The recent RHIC run with Au–Au collisions at $\sqrt{s_{\rm NN}} = 62.4$ GeV allows the measurement of the nuclear modification factor for charged hadrons and neutral pions up to transverse momenta of 7–8 GeV. We estimate the leading-

$\langle \hat{q} \rangle \propto n^{\rm gluons} \propto {\rm A}^{0.383} \left(\sqrt{s_{\rm NN}}\right)^{0.574}$

$n^{\rm gluons}_{\rm Au-Au,\,62.4\,GeV} \simeq 0.5 \times n^{\rm gluons}_{\rm Au-Au,\,200\,GeV}$

$\langle \hat{q} \rangle \simeq 7\ {\rm GeV}^2/{\rm fm}$ in central collisions at 62.4 GeV.

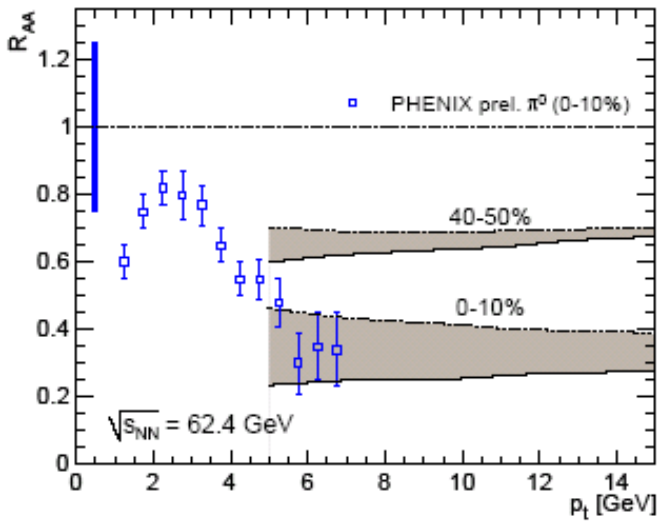

Figure 9: Model results for $R_{\rm AA}(p_{\rm t})$ in central and semi-peripheral Au–Au collisions at $\sqrt{s_{\rm NN}} = 62.4$ GeV. The preliminary π^0 data (0–10% centrality class) from PHENIX [35] are also shown; the pp reference is the PHENIX pp $\rightarrow \pi^0 + X$ parameterization, the error bars on the data points are the combined statistical and $p_{\rm t}$-dependent systematic errors and the bar centred at $R_{\rm AA} = 1$ is the systematic error on the normalization.

Extrapolation to the LHC (5.5 TeV)

$$n^{\text{gluons}}_{\text{Pb}-\text{Pb},\,5.5\,\text{TeV}} \simeq 7 \times n^{\text{gluons}}_{\text{Au}-\text{Au},\,200\,\text{GeV}}, \text{ i.e. } \langle \hat{q} \rangle \simeq 100\ \text{GeV}^2/\text{fm}.$$

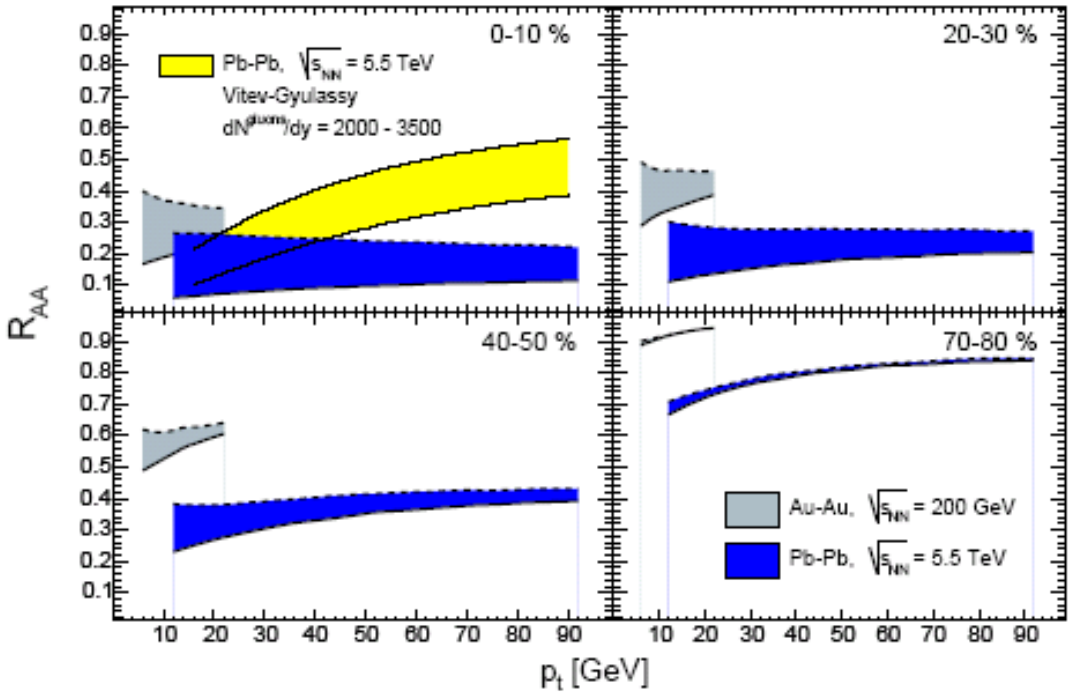

Figure 10: $R_{\mathrm{AA}}(p_{\mathrm{t}})$ for different centrality classes in Pb–Pb collisions at $\sqrt{s_{\mathrm{NN}}} = 5.5$ TeV and in Au–Au collisions at $\sqrt{s_{\mathrm{NN}}} = 200$ GeV. For comparison, the prediction for LHC presented in Ref. [17] (Vitev–Gyulassy) is also shown.

Section 5

Discussion

High-energy partons from the surface

$$n^{\text{gluons}}_{\text{Pb-Pb, 5.5 TeV}} \simeq 7 \times n^{\text{gluons}}_{\text{Au-Au, 200 GeV}}, \text{ i.e. } \langle \hat{q} \rangle \simeq 100 \text{ GeV}^2/\text{fm}.$$

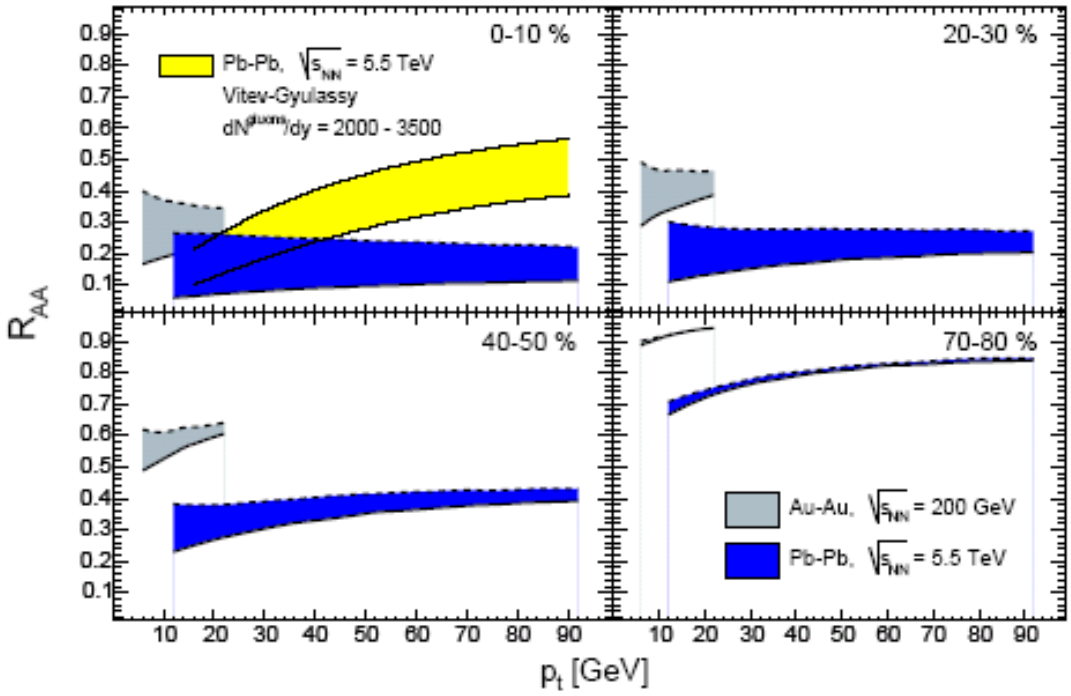

Figure 10: $R_{\mathrm{AA}}(p_{\mathrm{t}})$ for different centrality classes in Pb–Pb collisions at $\sqrt{s_{\mathrm{NN}}} = 5.5$ TeV and in Au–Au collisions at $\sqrt{s_{\mathrm{NN}}} = 200$ GeV. For comparison, the prediction for LHC presented in Ref. [17] (Vitev–Gyulassy) is also shown.

High-energy partons from the surface

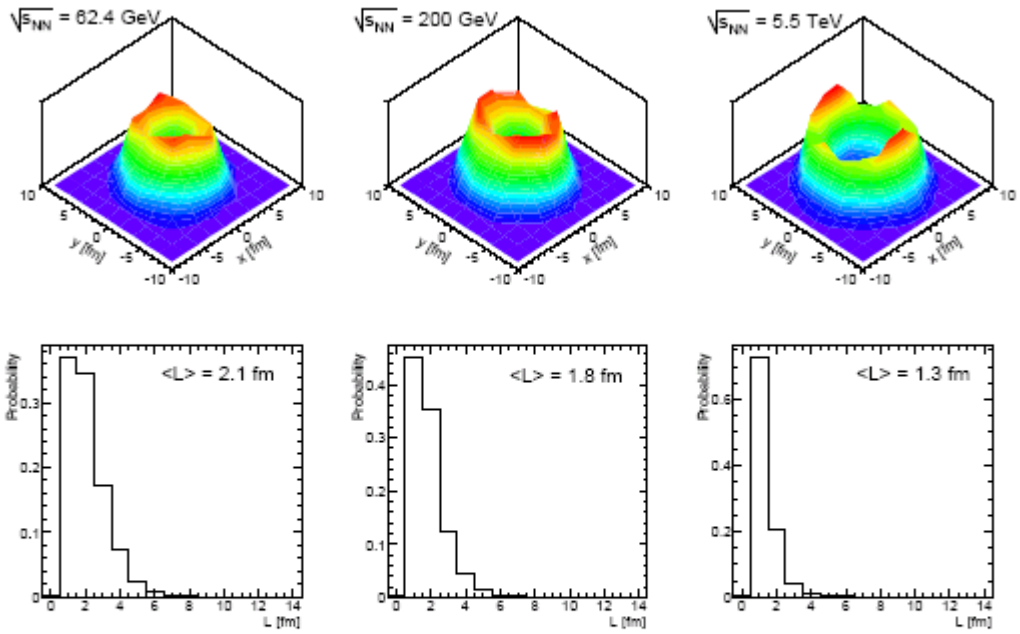

Figure 11: Distributions of parton production points in the transverse plane (upper row) and in-medium path length (lower row) for partons that escape the medium and produce hadrons with $p_t > 5$ GeV in central Au–Au collisions at 62.4 and 200 GeV and in central Pb–Pb collisions at 5.5 TeV. The quantity $\langle L \rangle$ is the average of the path length distribution. These plots were obtained in the *non-reweighted* approach.

It is interesting to try to apply a simple toy model: all partons with a path length L smaller than a maximum length $L_{\text{escape}}^{\text{max}}$ escape from the medium, the others are absorbed. We define the path length probability distribution $\mathcal{P}(\ell)$ as the probability distribution for a generic parton to have a

Energy loss saturation

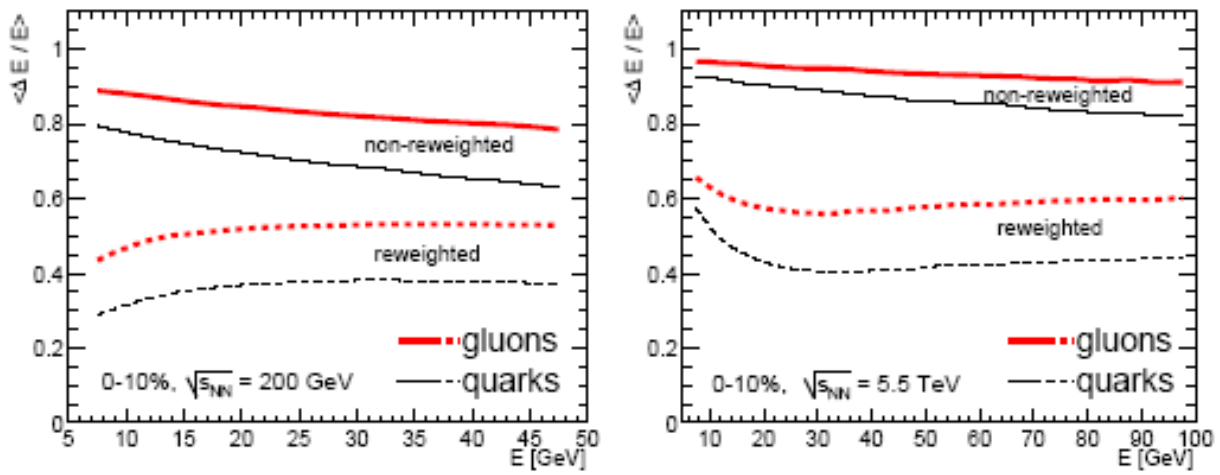

Figure 13: Average relative energy loss versus parton energy for quarks and gluons in central collisions at RHIC and LHC energies for the *non-reweighted* and *reweighted* cases.

Section 6

Conclusion

Energy loss saturation

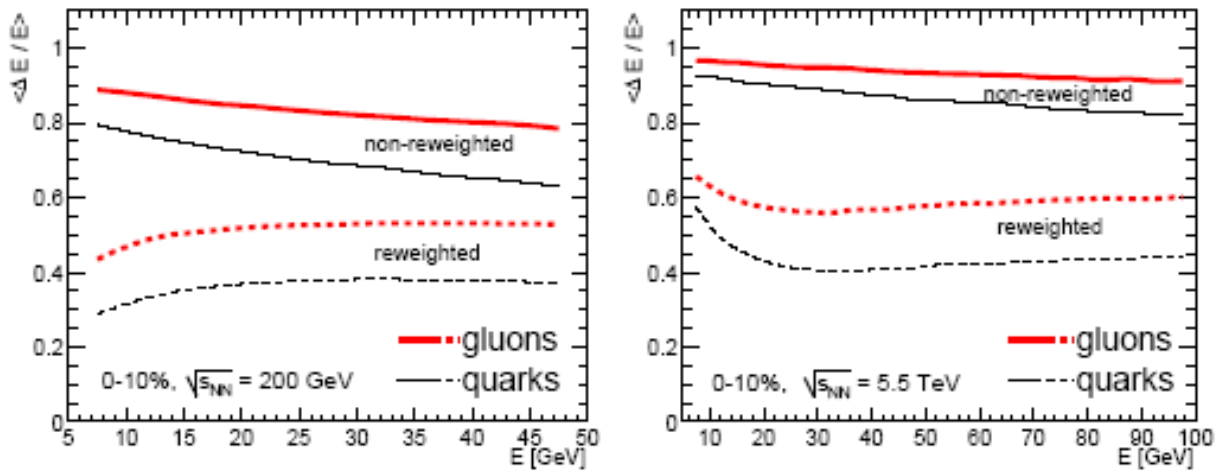

Figure 13: Average relative energy loss versus parton energy for quarks and gluons in central collisions at RHIC and LHC energies for the *non-reweighted* and *reweighted* cases.

Summary

(1/3). Due to the scaling $\Delta E \propto \alpha_s \hat{q}$, if larger values (e.g. 1/2) were used, the extracted transport coefficient would be smaller, but still quite large, $\langle \hat{q} \rangle \simeq 10$ GeV^2/fm [22]. In Ref. [22], it is pointed out that such $\hat{q}$ values do not necessarily imply unexpectedly large medium initial energy densities (a few hundreds GeV/fm^3), as one obtains in the hypothesis of an ideal plasma whose constituents interact perturbatively with the hard partons [15], but rather suggest that the medium might interact with the hard partons much stronger than perturbatively expected. Technically, the large extracted $\hat{q}$